

Study of stability of luminescence intensity of β -NaGdF₄:Yb:Er nanoparticle colloids in aqueous solution

I. D. Kormshchikov^{1,2}, V. V. Voronov¹, S. A. Burikov³, T. A. Dolenko³, S. V. Kuznetsov^{1,*}

¹Prokhorov General Physics Institute of the Russian Academy of Sciences,
Vavilov str, 38, Moscow, 119991 Russia

²Faculty of Chemistry, Moscow State University, Moscow, 119991 Russia

³Faculty of Physics, Moscow State University, Moscow, 119991 Russia

*kouznetzovsv@gmail.com

DOI 10.17586/2220-8054-2021-12-2-218-223

Hexagonal modification β -NaGdF₄:Yb:Er with a particle size of 24 nm was synthesized by the solvothermal technique. Concentrated aqueous colloids of nanoparticles were prepared using polyvinylpyrrolidone as the surfactant. The study of the luminescence characteristics for 25 days revealed that the luminescence intensity did not significantly change and hydrolysis of nanoparticles was not observed.

Keywords: nanofluoride, up-conversion luminescence, luminescence stability of the aqueous colloid.

Received: 15 February 2021

Revised: 10 April 2021

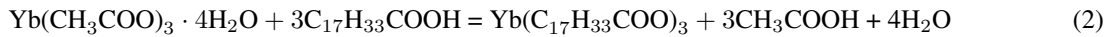
1. Introduction

The development of bioimaging allows *in vivo* determination of the impact of pharmaceuticals on cells. Dyes [1–3], quantum dots [1, 2], carbon nanoparticles [3–7] and up-conversion luminescence fluoride nanoparticles [1, 8, 9] are used as biosensors. Fluorides possess chemical stability and high values for up-conversion luminescence quantum yields [10–12]. Up-conversion luminescence is convenient for bioimaging, since it allows the excitation of the phosphor in the near-infrared region of the spectrum and the registration of the luminescence response in the visible range of the spectrum [13, 14]. Various techniques have been developed which allow *in vivo* determination of temperature [15–18], pH, and a viscosity [19] inside cells based on up-conversion nanoparticles. The highest quantum yields of up-conversion luminescence (PLQY) were recorded for β -NaYF₄:21.4%Yb³⁺, 2.2%Er³⁺ (PLQY=10.5% at 35 W/cm²) [20], BaY₂ZnO₅:7%Yb³⁺, 3%Er³⁺ (PLQY=5% at 2.2 W/cm²) [21], La₂O₂S:9%Yb³⁺, 1%Er³⁺ (PLQY=5.8% at 13 W/cm²) [22], SrF₂:3%Yb, 2%Er (PLQY=6.5% at 230 W/cm²) [11]. Instead of the NaYF₄ matrix, NaGdF₄ is being actively investigated, since gadolinium, in comparison to yttrium, is an NMR, X-ray, and photosensitive ion [23]. Cell-based research requires aqueous colloids of nanoparticles demonstrating stable luminescent characteristics. One of the effective luminescence quenchers is hydroxyl ion, which lead to the hydrolysis of nanoparticles. Hydrolysis study of the nanoparticles through the stages of formation of hydroxides and oxides was carried out in [24] based on HAADF-TEM for CaF₂:Yb nanoparticles to explain the source of optical losses in optical ceramics. From a chemical point of view, the scenario of obtaining oxofluorides rather than hydroxides is more probable due to the significant difference between the rates of hydrolysis of rare earth, alkaline, and alkaline earth fluorides [25, 26]. An illustrative example is the BaF₂-BiF₃ system, for which it is impossible to obtain bismuth fluoride by precipitation from aqueous solutions [27]. Stability of the luminescence characteristics, possibility of hydrolysis under the action of laser pumping, hydration of the nanoparticle surface in aqueous solutions are important questions at investigation of luminescence characteristics of aqueous colloids of nanoparticles. Decrease in the luminescence intensity during exposure of nanoparticles in aqueous solutions due to hydrolysis processes, which can be prevented by using a NaF as a buffer or organic or inorganic shell [28, 29]. Colloid measurements are often limited to a few days, which make it impossible to estimate the reproducibility of the measured data. Finally, the task of comparing the nanoparticles' luminescent characteristics becomes much more complicated. In our research, aqueous colloids of β -NaGdF₄:Yb:Er nanoparticles were synthesized and the stability of their luminescent characteristics was studied with an unchanged optical scheme for 25 days. It was reliably shown that the luminescence intensity of colloids does not change and the absence of the influence of the hydrolysis impact on the luminescence characteristics.

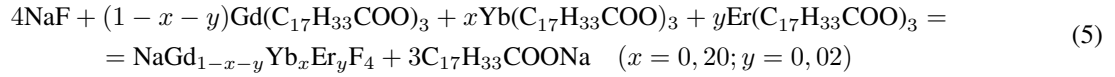
2. Experimental part

Gadolinium, ytterbium, and erbium acetates with a purity of 99.99 (LANHIT, Russia), ammonium fluoride, and sodium hydroxide (chemically pure, Chimmed), octadecene-1 (90%, VEKTON), oleic acid (pure, Chimmed) were used as initial chemicals.

The synthesis of β -NaGdF₄:Yb:Er nanoparticles were carried out in several stages as described in [30]. In the first step, 1.2199 g Gd(CH₃COO)₃·4H₂O, 0.3249 g of Yb(CH₃COO)₃·4H₂O, and 0.0321 g of Er(CH₃COO)₃·4H₂O were placed in a 250 ml three-necked flask with a reflux condenser, and oleic acid (10.9 ml) and octadecene-1 (58 ml) were added. The system was filled with argon after preliminary evacuation. The reaction mixture was heated to 130 °C with stirring until the solid acetates were completely dissolved. Then, water and acetic acid were removed by vacuum pumping with control until foaming ceased. At this stage, RE oleates were synthesized by reactions (1-3).



In the second step, the formed oleates were fluorinated with α -NaGdF₄:Yb:Er nanoparticles formation with a cubic crystal structure by reaction (4-5).



Appropriate weights of NaOH (0.1540 g) and NH₄F (0.5698 g) were dissolved in methanol and was added to the reaction mixture with oleates at room temperature. The reaction mixture was heated to 50–60 °C for methanol removal during vacuum pumping. The removal of all methanol was monitored by the end of the foaming of the solution. The resulting reaction mixture was held for 1 hour at 60 °C to nucleate nanoparticles of a cubic metastable modification. In the third step, the polymorphic transformation from the cubic into the hexagonal phase was carried out at 290–300 °C for 1.5 hours. The choice of temperature 290–300 °C is due to the phase transition from the cubic to the hexagonal phase.

Nanoparticles were isolated by centrifugation (7000 rpm, 6 min). The precipitate was washed three-times in chloroform with intermediate centrifugation. Aqueous solutions of nanoparticle colloids were prepared in two stages using polyvinylpyrrolidone (PVP) as a surfactant. Sodium-gadolinium nanofluorides are insoluble in water and poorly dispersed indirect interaction with water. Appropriate weighed quantities of β -NaGdF₄:Yb:Er nanoparticles were dispersed in chloroform and sonicated for 20 minutes at room temperature. An aqueous solution of PVP (1 wt.% or 2 wt.%) was slowly added dropwise to a suspension of β -NaGdF₄:Yb:Er nanoparticles in chloroform under vigorous stirring. The resulting mixture was kept in an ultrasonic bath at 63 °C to remove chloroform (boiling point 61.2 °C) for colloid formation. Control of the completeness of chloroform removal was carried out by changing the volume of the solution. X-ray powder diffraction analysis was performed on a Bruker D8 Advance diffractometer (from 12 to 55 2 θ with 0.02 2 θ step) with CuK α radiation. The unit cell parameters were calculated using the Powder 2.0 software (calculation error $\Delta Q < 10$), where $\Delta Q = 10^4/d_{theor}^2 - 10^4/d_{calc}^2$, d is the interplanar distance. The coherent scattering region was calculated using the Scherrer formula. Transmission electron microscopy was performed on a JEOL JEM-2100 microscope. The particle size was estimated using the ImageJ software. Energy dispersive analysis (EDX) was performed on a Carl Zeiss NVision 40 microscope.

The photoluminescence spectra of β -NaGdF₄:Yb:Er nanoparticles were obtained in the 90-degree geometry on a setup consisting of a pulsed laser (Solar LS, 980 nm excitation, pulse duration 12 ns, pulse repetition rate 100 Hz, average power density 3.4 MW/cm² or 40.7 mJ/cm² in impulse), monochromator (MVR-80, focal length 500 mm, diffraction grating 600 lines/mm) and a CCD camera (1024 * 128 Synapse BIUV, Horiba Jobin Yvon).

3. Results and discussion

A typical X-ray diffraction pattern of synthesized β -NaGdF₄:Yb:Er solid solution is shown in Fig. 1. Comparison with JCPDS 27-0699 for hexagonal modification β -NaGdF₄ revealed complete agreement of the X-ray diffraction reflections with a slight shift in the peak positions. The deviation of the calculated unit cell parameters $a = 5.981(6)$, $c = 3.63(2)$ Å from the JCPDS 27-0699 data ($a = 6.020$ Å, $c = 3.601$ Å) arise from a difference in the sizes of the gadolinium, ytterbium, and erbium ions [31]. The coherent scattering region was 12 nm.

The transmission electron microscopy (TEM) image is presented in Fig. 2. The particles have average size of about 24 nm. TEM image and coherent scattering region allows us to conclude that nanoparticles grow by cooperative growth mechanism [32].

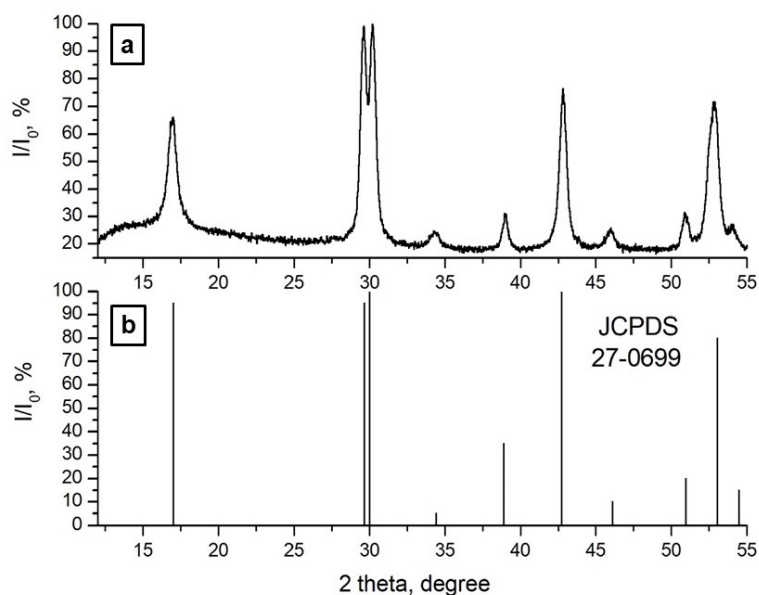


FIG. 1. X-ray diffraction patterns of (a) β -NaGdF₄:Yb:Er and (b) JCPDS 27-0699

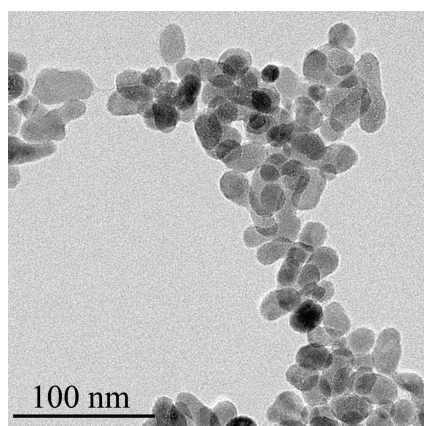


FIG. 2. Transmission electron microscopy of β -NaGdF₄:Yb:Er nanoparticles

The actual composition was determined by EDX as Na_{1,186}Gd_{0,606}Yb_{0,192}Er_{0,016}F_{3,628}, while the nominal composition was NaGd_{0,78}Yb_{0,20}Er_{0,02}F_{4,00}. The distribution coefficients (k) were: $k(\text{Na})= 1.19$, $k(\text{Gd})= 0.78$, $k(\text{Yb})= 0.96$, $k(\text{Er})= 0.80$, which means there is an incongruent crystallization of the powders.

The aqueous colloids with different concentrations of nanoparticles and PVP were prepared (Table 1).

TABLE 1. Concentration of β -NaGdF₄:Yb:Er colloids

Sample	Colloid concentration, mg/ml	PVP, wt.%
1	1.0	1.0
2	1.0	2.0
3	2.0	1.0
4	2.0	2.0

The luminescence spectra with excitation at 980 nm on the first day of the experiment are presented in Fig. 3. The luminescence spectra of colloids contain luminescence bands with maxima at 522 nm, 544 nm and 655 nm, which correspond to the transitions $^2\text{H}_{11/2} \rightarrow ^4\text{I}_{15/2}$, $^4\text{S}_{3/2} \rightarrow ^4\text{I}_{15/2}$, $^4\text{F}_{9/2} \rightarrow ^4\text{I}_{15/2}$ of the erbium ion. Analysis of the

luminescence spectra revealed that an increase of nanoparticles concentration from 1.0 to 2.0 mg/ml led to an increase in the luminescence intensity in ten times at the same PVP content (1.0 wt.%). An increase in the PVP content up to 2.0 wt.% at a particle concentration of 2.0 mg/ml resulted in a decrease in the luminescence intensity by two-fold, which is associated with an increase in scattering due to the appearance of turbidity of the colloid. An increase in the luminescence intensity of samples with increase in the PVP content from 1.0 to 2.0 wt.% at the same nanoparticle content of 1 mg/ml was associated with the prevention of luminescence quenching processes due to the interaction of hydroxyl ions with surface of nanoparticles. The effect of an aqueous medium on the luminescence intensity was analyzed based on sample 3, which demonstrated the most intense luminescence and low solution turbidity. This sample has a low PVP concentration, which does not prevent the interaction of water with the nanoparticle surface.

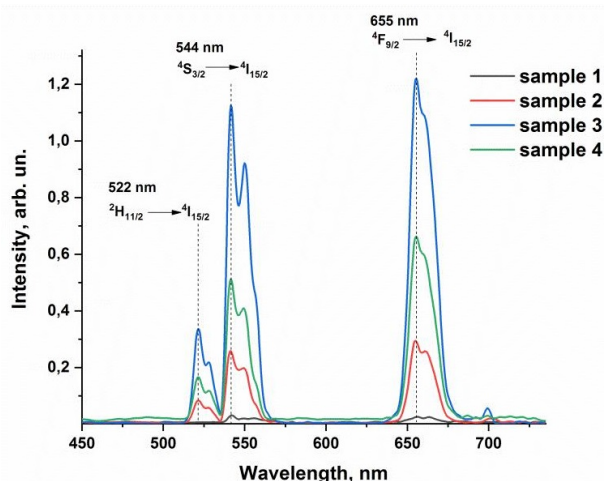


FIG. 3. Luminescence spectra of β -NaGdF₄:Yb:Er aqueous colloids on the first day of the experiment

Studying the luminescent properties of nanoparticle suspensions complicated by elastic scattering. This contribution is expressed in a decrease in the luminescence intensity and distortion of the shape of its spectra. Strong scattering at the exciting radiation wavelength effectively reduces the power density of the probe radiation in the signal collection region, which leads to a decrease in the luminescence intensity. The signal intensity also decreases directly due to the scattering of luminescence photons. Since the scattering efficiency depends on the wavelength, the shape of the spectra is also distorted. In the case of small particles (less than the radiation wavelength), the dependence of the scattering intensity on the wavelength obeys the $1/\lambda^4$ law. If the scattering intensity increases due to an increase in the particle size due to aggregation, the spectra are distorted i.e. the ratios between the intensities of the luminescence bands change. Control of the possible contribution of scattering to the change in the luminescence spectra was revealed by calculation of band intensities ratios in the region of 540 nm and 520 nm. Decrease in this ratio would indicate an increase in scattering. A clear tendency to change this ratio with time was not found (Fig. 4), which indicates that the intensity of radiation scattering remains unchanged within the framework of this experiment.

The luminescence spectra were recorded regularly for 25 days. The results are presented in the form of histograms characterizing the change in the integral intensity of the luminescence bands in the 496–583 nm and 636–689 nm ranges (Fig. 5). The reproducibility of luminescence spectra during a measuring day was ensured by repeating the measurement 5 times. Reproducibility of luminescence spectra was about 10%. Finally, the mean value and standard deviation were calculated. Analysis of the histograms did not demonstrate the change in luminescent characteristics within 25 days. This indicates the absence of hydrolysis processes on the surface of nanoparticles and the possible compatibility of using aqueous colloids of β -NaGdF₄:Yb:Er nanoparticles for long-term biomedical research.

4. Conclusion

Nanoparticles of β -NaGdF₄:Yb:Er were synthesized by the solvothermal technique. Based on the data on the coherent scattering region (12 nm) and transmission electron microscopy (24 nm), it is shown that the growth of nanoparticles occurs by the cooperative growth mechanism. Stable colloidal solutions of nanoparticles with a concentration of 1–2 mg/ml were prepared by using polyvinylpyrrolidone as a surfactant. Measurement of the luminescence

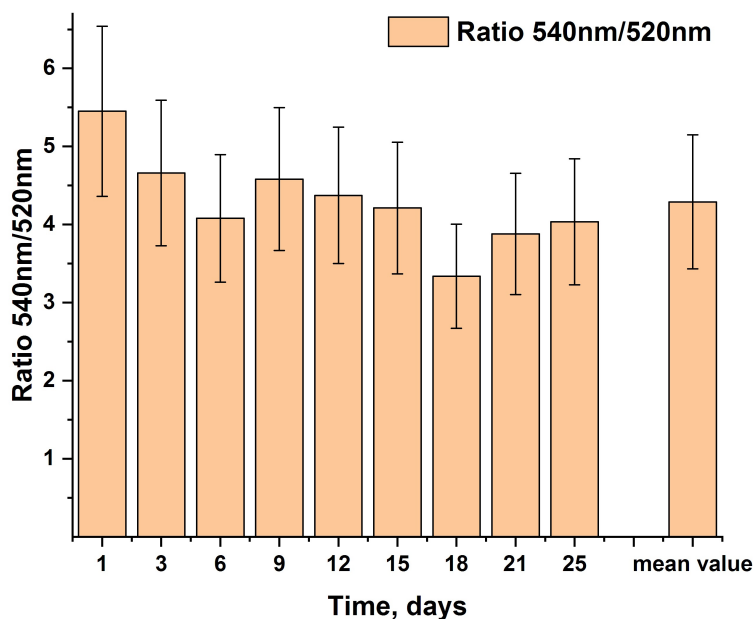


FIG. 4. The ratio of band intensities in the region of 540 nm and 520 nm on different days

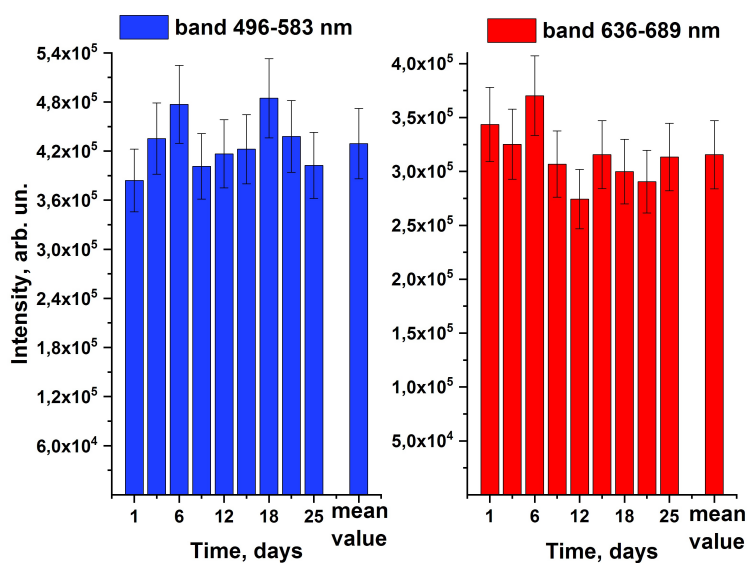


FIG. 5. Intensities of the luminescence bands of the aqueous colloid of β -NaGdF₄:Yb:Er in 496–583 nm and 636–689 nm ranges over a 25 day period

spectra for 25 days revealed the retention of the luminescence intensity at the level of measurement error. This indicates the possibility of using such colloids for biomedical applications and the absence of intense hydrolysis of nanoparticles.

Acknowledgements

Authors thanks to Tabachkova N. Yu. for transmission electron microscopy.

References

- [1] Wolfbeis O.S. An overview of nanoparticles commonly used in fluorescent bioimaging. *Chem. Soc. Rev.*, 2015, **44**, P. 4743–4768.
- [2] Fei X., Gu Y. Progress in modifications and applications of fluorescent dye probe. *Progress in Natural Science*, 2009, **19**, P. 1–7.
- [3] Fan J.Y., Chu P.K. Group IV Nanoparticles: Synthesis, properties, and biological applications. *Small*, 2010, **6**, P. 2080–2098.

- [4] Khan W.U., Wang D., Wang Y. Highly Green Emissive Nitrogen-Doped Carbon Dots with Excellent Thermal Stability for Bioimaging and Solid-State LED. *Inorganic Chemistry*, 2018, **57**, P. 15229–15239.
- [5] Molaei M.J. Carbon quantum dots and their biomedical and therapeutic applications: a review. *RSC Advances*, 2019, **9**, P. 6460–6481.
- [6] Rosenholm J.M., Vlasov I.I., Burikov S.A., Dolenko T.A., Shenderova O.A. Nanodiamond-Based Composite Structures for Biomedical Imaging and Drug Delivery (Review). *J. of Nanoscience and Nanotechnology*, 2015, **15**, P. 959–971.
- [7] Sarmanova O.E., Burikov S.A., Dolenko S.A., Isaev I.V., Laptinskiy K.A., Prabhakar N., Karaman D.S., Rosenholm J.M., Shenderova O.A., Dolenko T.A. A method for optical imaging and monitoring of the excretion of fluorescent nanocomposites from the body using artificial. *Nanomedicine: Nanotechnology, Biology, and Medicine*, 2018, **14**, P. 1371–1380.
- [8] Rodríguez-Sevilla P., Sanz-Rodríguez F., Peláez R.P., Delgado-Buscalioni R., Liang Liangliang, Liu Xiaogang, Jaque Daniel. Single-cell diagnosis by upconverting nanorockers. *Advanced Biosystems*, 2019, **3**, P. e1900082.
- [9] Wua Wei, Wanga Xian, Tiana Yuexing, Wanga Shasha, Deab Gejihu. Controlled synthesis and luminescent properties of Ca_{0.80}Yb_{0.20}F_{2.2}: 0.2% Tm³⁺ nanocrystals. *J. Fluor.Chem.*, 2021, **242**, P. 109696.
- [10] Fedorov P.P., Kuznetsov S.V., Osiko V.V. Elaboration of nanofluorides and ceramics for optical and laser applications. Chapter in the book *Photonic and Electronic Properties of Fluoride Materials*. Ed. A.Tressaud, K. Poeppelmeier, Print Book, 2016, P. 7-31.
- [11] Reig David Saleta, Grauel Bettina, Konyushkin V.A., Nakladov A.N., Fedorov Pavel P., Busko Dmitry, Howard Ian Arthur, Richards Bryce S., Resch-Genger Ute, Kuznetsov Sergey, Turshatov Andrey, Würth Christian. Upconversion properties of SrF₂:Yb³⁺,Er³⁺ single crystals. *J. Mater. Chem. C.*, 2020, **8**, P. 4093–4101.
- [12] Ermakova Yu.A., Pominova D.V., Voronov V.V., Kuznetsov S.V. Algorithm for calculation of up-conversion luminophores mixtures chromaticity coordinates. *J. Fluor. Chem.*, 2020, **237**, P. 109607.
- [13] Pominova D.V., Romanishkin I.D., Proydakova V.Yu., Grachev P.V., Moskalev A.S., Ryabova A.V., Makarov V.I., Linkov K.G., Kuznetsov S.V., Uvarov O.V., Loschenov V.B. Comparison of 920, 940 and 970 nm wavelengths in terms of penetration depth and thermal effects on biological tissues as well as up-conversion luminescence excitation efficiency. *Methods Appl. Fluoresc.*, 2020, **8**, P. 025006.
- [14] Liu W., Chen R., He S. Ultra-stable near-infrared Tm³⁺-doped upconversion nanoparticles for in vivo wide-field two-photon angiography with a low excitation intensity. *Journal of Innovative Optical Health Sciences*, 2019, **12**, P. 1950013.
- [15] Brites C.D.S., Balabhadra S., Carlos L.D. Lanthanide-based thermometers: at the cutting-edge of luminescence thermometry. *Adv. Opt. Mater.*, 2019, P. 71801239.
- [16] Jaque D., Vetrone F. Luminescence nanothermometry. *Nanoscale*, 2012, **4**, P. 4301–4326.
- [17] Brites C.D.S., Kuznetsov S.V., Konyushkin V.A., Nakladov A.N., Fedorov P.P., Carlos L.D. Simultaneous measurement of the emission quantum yield and local temperature: the illustrative example of SrF₂:Yb³⁺/Er³⁺ single crystals. *Eur. J. Inorg. Chem.*, 2020, **2020**, P. 1555–1561.
- [18] Sarmanova O.E., Burikov S.A., Laptinskiy K.A., Kotova O.D., Filippova E.A., Dolenko T.A. In vitro temperature sensing with up-conversion NaYF₄:Yb³⁺/Tm³⁺-based nanocomposites: peculiarities and pitfalls. *Spectrochimica Acta Part A: Molecular and Biomolecular Spectroscopy*, 2020, **241**, P. 118627(8 p).
- [19] Sevilla Paloma Rodríguez, Rodríguez Francisco Sanz, Pelez Raúl P., Buscalioni Rafael Delgado, Liang Liangliang, Liu Xiaogang, Jaque Daniel. Upconverting Nanorockers for Intracellular Viscosity Measurements During Chemotherapy. *Advanced in Biosystems*, 2019, **3**, P. 1900082.
- [20] Kaiser M., Wurth C., Kraft M., Hyppanen I., Soukka T., Resch-Genger U., *Nanoscale*, 2017, **9**, P. 10051–10058.
- [21] Etchart I., Huignard A., Berard M., Nordin M.N., Hernandez I., Curry R.J., Gillin W.P., Cheetham A.K. *J. Mater. Chem.*, 2010, **20**, P. 3989–3994.
- [22] Pokhrel M., Kumar G.A., Sardar D.K. *J. Mater. Chem. A*, 2013, **1**, P. 11595–11606.
- [23] Yu Songxia, Wang Zhiqiang, Cao Ruijun, Meng Lingjie. Microwave-assisted synthesis of water-disperse and biocompatible NaGdF₄:Yb,Ln@NaGdF₄ nanocrystals for UCL/CT/MR multimodal imaging. *J. Fluor. Chem.*, 2017, **200**, P. 77–83.
- [24] Lyberis A., Patriarche G., Gredin P., Vivien D., Mortier M. Origin of light scattering in ytterbium doped calcium fluoride transparent ceramic for high power lasers. *J. Eur. Ceram. Soc.*, 2011, **31**, P. 1619–1630.
- [25] Warf J.C., Cline W.C., Tevebaugh R.D. Pyrohydrolysis in Determination of Fluoride and Other Halides. *Analytical Chemistry*, 1954, **26**, P. 342–346.
- [26] Banks C.V., Burke K.E., O'Laughlin J.W. The determination of fluorine in rare-earth fluorides by high temperature hydrolysis. *Analytica Chimica Acta*, 1958, **19**, P. 230–243.
- [27] Fedorov P.P., Mayakova M.N., Kuznetsov S.V., Voronov V.V., Osiko V.V., Ermakov R.P., Gontar' I.V., Timofeev A.A., Iskhakova L.D. Coprecipitation of barium-bismuth fluorides from aqueous solutions: Nanochemical effects. *Nanotechnologies in Russia*, 2011, **6**, P. 203–210.
- [28] Dukhno O., Przybilla F., Muhr V., Buchner M., Hirsch T., Mely Y. Time-dependent luminescence loss of individual upconversion nanoparticles upon dilution in aqueous solutions. *Nanoscale*, 2018, **10**, P. 15904–15910.
- [29] Andresen E., Würth C., Prinz C., Michaelis M., Resch-Genger U. Time-resolved luminescence spectroscopy for monitoring the stability and dissolution behaviour of upconverting nanocrystals with different surface coatings. *Nanoscale*, 2020, **12**, P. 12589–12601.
- [30] Li Zhengquan, Zhang Yong. An efficient and user-friendly method for the synthesis of hexagonal-phase NaYF₄:Yb, Er/Tm nanocrystals with controllable shape and upconversion fluorescence. *Nanotechnology*, 2008, **19**, P. 345606.
- [31] Shannon R.D. Revised effective ionic radii and systematic studies of interaction distance in halides and chalcogenides. *Acta Crystallogr. A*, 1976, **32**, P. 751–767.
- [32] Ivanov V.K., Fedorov P.P., Baranchikov A.Y., Osiko V.V. Oriented aggregation of particles: 100 years of investigations of non-classical crystal growth. *Russ. Chem. Rev.*, 2014, **83**, P. 1204–1222.